

# Chemical-looping combustion and chemical-looping reforming of kerosene in a circulating fluidized-bed 300 W laboratory reactor

Patrick Moldenhauer<sup>a,\*</sup>, Magnus Rydén<sup>a</sup>, Tobias Mattisson<sup>a</sup>, Anders Lyngfelt<sup>a</sup>

<sup>a</sup>Department of Energy and Environment, Division of Energy Technology, Chalmers University of Technology, S-412 96 Göteborg, Sweden

## Abstract

The reaction between a nickel-based oxygen carrier and a liquid fuel has been demonstrated in a chemical-looping reactor with continuous particle circulating. An injection system was constructed, in which sulphur-free kerosene was evaporated, mixed with superheated steam and fed directly into the lab scale chemical-looping reactor. A nickel-based oxygen carrier composed of 40 wt% NiO and 60 wt% MgO-ZrO<sub>2</sub> was used for both chemical-looping combustion (CLC) and chemical-looping reforming (CLR) experiments, which were performed for about 34 h and 20 h, respectively. For the CLC experiments, 95–99 % of the fuel carbon was converted to CO<sub>2</sub> and only a minute amount of hydrocarbons was detected in the off-gas. For the CLR experiments, synthesis gas was produced with concentrations of hydrocarbons as low as 0.01 %. The particles were analyzed before and after the experiments using XRD, SEM, BET surface area and particle size distribution.

It was shown that it is possible to use liquid fuel in a continuous chemical-looping process and also achieve nearly complete fuel conversion. With a nickel-based oxygen carrier virtually all hydrocarbon could be fully oxidized.

**Keywords:** chemical-looping combustion (CLC), chemical-looping reforming (CLR), liquid fuel, kerosene, nickel-based oxygen carrier, circulating fluidized bed (CFB), CO<sub>2</sub> capture

## 1. Introduction

Chemical-looping processes have been investigated thoroughly with gaseous and solid fuels. Recent overviews over developments, advancements and operational experience in chemical-looping were given in 2008 by Hossain and de Lasa [1], in 2009 by Fang et al. [2] and in 2010 by Lyngfelt [3]. However, only a handful of articles have been published that focus on the use of liquid fuels in chemical-looping applications. Pimenidou et al. used waste cooking oil in a batch packed bed reactor in order to produce a synthesis gas, using a nickel-based oxygen carrier [4]. High purity hydrogen was produced by adding calcined dolomite as CO<sub>2</sub> sorbent into the catalytic bed [5]. Cao et al. gasified bitumen and asphalt in a separate pyrolysis unit before feeding the synthesis gas into a batch fluidized-bed reactor with a copper-based oxygen carrier [6]. Forret et al. and Hoteit et al. conducted chemical-looping combustion experiments, where liquid fuel was injected into a batch fluidized-bed reactor with a nickel-based oxygen carrier. The investigated fuels included n-dodecane [7], a domestic fuel oil and a heavy fuel oil [8]. Mendiara et al. conducted a set of experiments where a flow of nitrogen was saturated with toluene, a synthesized tar, which was then fed into a fixed-bed reactor, using nickel-based, manganese-based and ilmenite oxygen carriers [9].

This study focuses on the direct use of liquid fuel in a continuous chemical-looping process. It is part of a project, sup-

ported by Saudi Aramco, with the title “Chemical-looping with liquid hydrocarbon fuels” and the final aim of utilizing heavy oil residues for production of heat and power.

Both chemical-looping combustion and synthesis gas generation by chemical-looping reforming were conducted in a 300 W circulating fluidized-bed laboratory reactor.

### 1.1. Chemical-Looping Combustion

Chemical-looping combustion (CLC) is a method of burning fuels with inherent separation of CO<sub>2</sub> [10]. In the most common CLC approach, particles are circulated between two interconnected fluidized-bed reactors, air reactor and fuel reactor, with no gas leakage between the reactors. In the air reactor (AR), the particles are oxidized with air, and in the fuel reactor (FR), they are reduced by fuel, before the cycle begins anew. As the oxygen carrier (OC) is circulated between air reactor and fuel reactors, it transports oxygen from the air to the fuel. Thus, air and fuel are never mixed and after condensing the water, the stream of flue gases consists of nearly pure CO<sub>2</sub>. The inherent separation of the CO<sub>2</sub> does not cause an energy penalty. High efficiency, high CO<sub>2</sub> capture rate and the possibility to use different kinds of fuels suggests that CLC could be economically feasible.

Figure 1 shows the basic design of a CLC system and illustrates the working principle. The reactions in air reactor and fuel reactor are expressed by reaction (1) and (2), respectively.

\*Corresponding author. Telephone: +46 (0)31-772 1469

Email address: patrick.moldenhauer@chalmers.se (Patrick Moldenhauer)

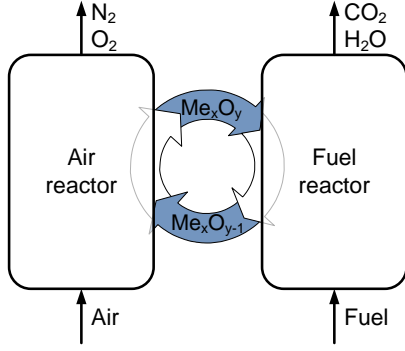
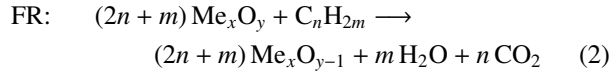
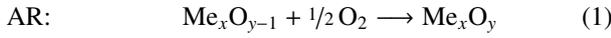


**Figure 1:** Schematic illustration of the chemical-looping combustion process

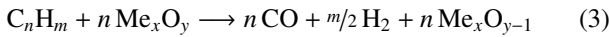


Here  $\text{Me}_x\text{O}_y$  denotes a metal oxide. The oxidation of the particles in the air reactor, see reaction (1), is exothermic. The reducing reaction in the fuel reactor, see reaction (2), can be either exothermic or endothermic, depending on the oxygen carrier material and the fuel used.

### 1.2. Chemical-Looping Reforming

Chemical-looping reforming (CLR) is a process derived from CLC. Just like in CLC, oxygen is transported between two reactors by solid oxygen carrier particles. The difference compared to CLC is that insufficient amounts of air are added to the air reactor to convert the fuel to  $\text{CO}_2$  and  $\text{H}_2\text{O}$ . Instead, the product is synthesis gas, consisting mainly of  $\text{CO}$  and  $\text{H}_2$  [11].

The reaction in the air reactor is the same as for CLC, see reaction (1). Typically all oxygen is taken up by the oxygen carrier so that the off-gas from the air reactor will consist almost completely of  $\text{N}_2$ . While it is unavoidable that some fuel is fully oxidized according to reaction (2), the major part is partially oxidized according to reaction (3). Figure 2 shows the working principle of CLR.



$\text{H}_2\text{O}$  or  $\text{CO}_2$  could be added to the fuel reactor in order to adjust the  $\text{H}_2/\text{CO}$  ratio in produced synthesis gas [12] in accordance with reactions (4) and (5), respectively.

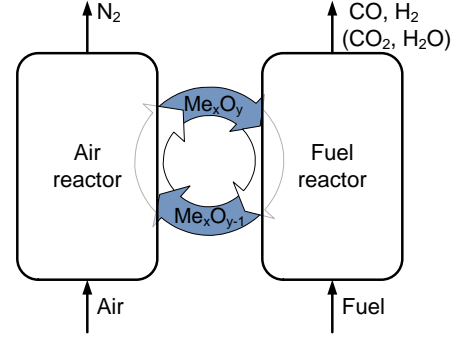
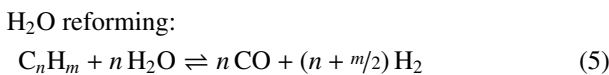
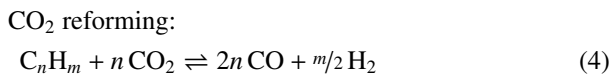
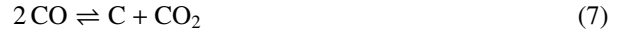


**Figure 2:** Schematic illustration of the chemical-looping reforming process

Both  $\text{H}_2\text{O}$  and  $\text{CO}_2$  also have the additional advantage of suppressing formation of solid carbon in the fuel reactor. The possibility for this is given through the substoichiometric condition in the fuel reactor. Solid carbon is likely to stem directly from the fuel through hydrocarbon decomposition, reaction (6). Another possible path for carbon deposition is the Boudouard reaction, reaction (7). At atmospheric chemical-looping operating conditions however, the Boudouard reaction is unlikely to go towards  $\text{C}$  unless the  $\text{CO}_2$  concentration is very low.



## 2. Experimental Details

### 2.1. 300 W Laboratory Reactor

An illustration of the reactor, which was used for the experiments of this work, is shown in Figure 3. A more detailed technical description can be found in [12].

Metal oxide particles enter the air reactor, where they are fluidized with air. During the fluidization reduced metal oxide particles ( $\text{Me}_x\text{O}_{y-1}$ ) are oxidized according to reaction (1). The fluidization velocity in the air reactor is high enough to create a circulating fluidized bed: while new particles are constantly fed to the bottom of the particle bed, particles at the top are accelerated upwards and leave the bed. The particle-gas mixture is then separated: the oxygen depleted air is returned to the atmosphere, whereas the metal oxide particles are transported through the upper loop-seal (downcomer) to the fuel reactor. There, the metal particles are reduced by fuel, which is also used to fluidize the particles. The reduced particles then pass through the lower loop-seal (slot) and return to the air reactor, where the whole cycle starts over again.

The 300 W reactor is subject to high heat losses due to a high surface-to-volume ratio. In order to achieve sufficiently high temperatures, typically  $750 - 950^\circ\text{C}$ , the reactor is encased in an electric furnace.

### 2.2. Fuel

The fuel was kerosene, which was provided by courtesy of Preem AB in Gothenburg, Sweden. By definition kerosene consists of different hydrocarbons with evaporation temperatures

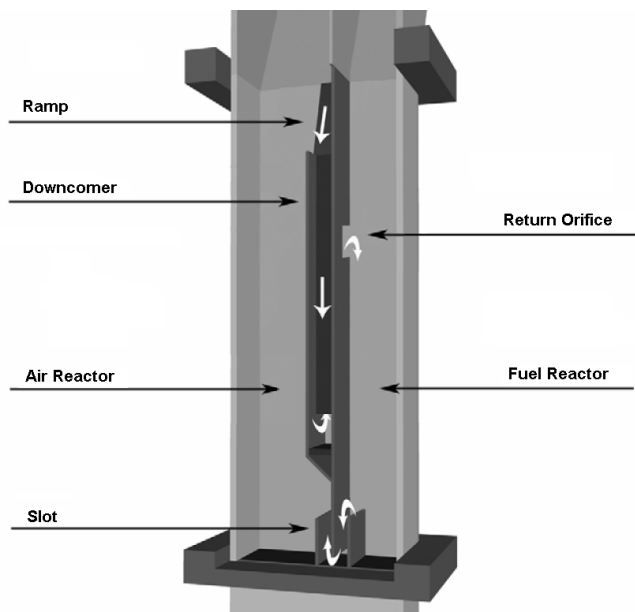


**Figure 3:** Schematic three-dimensional illustration of the 300 W laboratory reactor

between 150 °C and 320 °C. An elemental analysis showed a composition of 86.2 wt% carbon and 13.5 wt% hydrogen, which corresponds to a molar ratio H/C of 1.88. The lower heating value was determined to be 43.34 MJ/kg. It is likely that the fuel not only contains linear alkanes but also branched iso-alkanes and possibly even cyclic alkanes. The elemental analysis suggests the presence of arenes. Alkenes and alkynes are rather unlikely in mineral oil.

The fuel was also analyzed in a gas chromatograph (GC) and it was found that 99 wt% of the fuel content has an evaporation point below 250 °C and 80 wt% below 200 °C. Some of the peaks in the analysis coincided with those of linear alkanes. The most prominent ones were n-C10 (H/C = 2.20;  $T_{\text{boil}} = 174$  °C) and n-C11 (H/C = 2.18;  $T_{\text{boil}} = 196$  °C).

### 2.3. Injection Principle

The injection system was constructed and tested using the existing 300 W chemical-looping reactor, see Figure 3. The basic principle behind the injection system is to evaporate the liquid fuel using superheated steam as heat source and to inject the resulting gas mixture into the fuel reactor. This is most convenient, because it causes the least changes to the reactor system, which was designed for gaseous fuels, and thus reduces possible sources of error.

When the fuel molecules are converted the gas volume will increase. Hence, the volume flow of the gaseous steam-fuel mixture is a function of the extent of the hydrocarbon converted. The steam fulfils the secondary function of ensuring that enough gas is available to fluidize the particles in the fuel reactor. Poorly fluidized particles increase the risk of agglomeration, which may destroy the oxygen carrier batch, depending on the type of material used.

Figure 4 shows how evaporation, mixing and injection are realized. Steam is generated continuously by a steam genera-

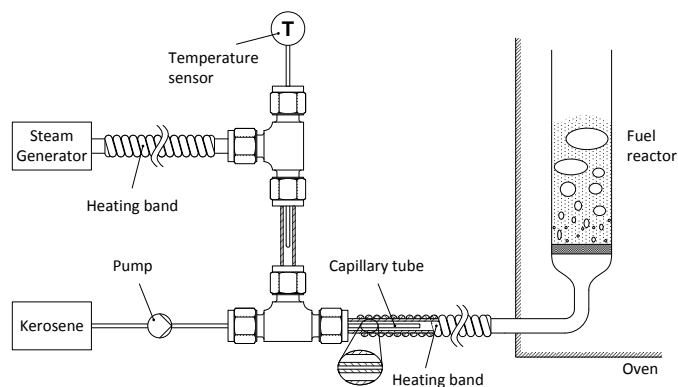


**Figure 4:** Schematic illustration of the injection principle for kerosene injection

tor. A heating band is used to superheat the steam to the desired temperature, which is measured by a thermocouple temperature sensor. A continuous fuel flow is provided by a diaphragm metering pump. The fuel is fed through a capillary tube, which is concentrically arranged within the steam pipe. The heat necessary for evaporation of the fuel is thereby transported from steam to fuel.

### 2.4. Measurements

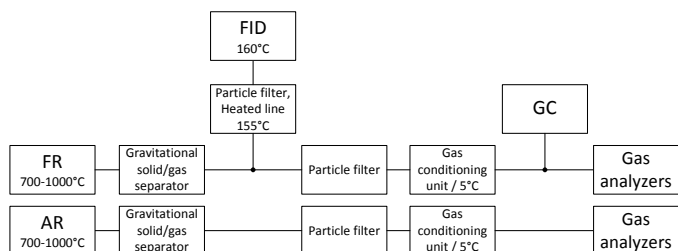


**Figure 5:** Schematic measurement layout

Figure 5 shows a schematic of the downstream gas measurements. The top part of the 300 W reactor is connected to a gravitational solid/gas separator, one for the air reactor (AR) and one for the fuel reactor (FR). Part of the hot flue gases of the fuel reactor are diverted and led through a heated line, at 155 °C, to a flame ionization detector (FID). The FID measures the content of organic carbon as CH<sub>4</sub> equivalent, without giving information about aromaticity or hydrogen content. The flue gases of both air reactor and fuel reactor are separately filtered and cooled down to 5 °C, before they pass through gas analyzers. The dry-gas content of CH<sub>4</sub>, CO and CO<sub>2</sub> is measured continuously by an IR analyzer and the content of O<sub>2</sub> by a paramagnetic sensor. Additionally, the dry fuel reactor gas is intermittently analyzed in a gas chromatograph (GC), which measures, besides the previously mentioned gases, H<sub>2</sub>, N<sub>2</sub>, and hydrocarbons up to C<sub>3</sub>H<sub>8</sub>. The GC used is equipped with two columns, Molsieve MS5Å 10 m × 0.32 mm (ID) and PorapLOT Q 10 m × 0.15 mm (ID), in which the gas sample is injected in parallel.

In addition to the analysis of the in situ data, X-ray powder diffractometry (XRD), density measurements and measure-

ments of the BET surface area (through gas adsorption) were performed with particles before and after the experiments.

### 2.5. Oxygen Carrier

The oxygen carrier used, N4MZ-1400, consists of 40 wt% NiO supported on 60 wt% Mg-stabilized ZrO<sub>2</sub>. The particles were produced through freeze-granulation with subsequent calcination at 1400 °C. The reactor was initially filled with 250 g of N4MZ-1400 particles in the size range of 90–212 μm. Particles from the same batch have been used for previous CLC and CLR experiments [13]. These experiments were performed both in a batch reactor with methane as fuel and in the 300 W reactor with natural gas as fuel. N4MZ-1400 was found to be a good oxygen carrier with high reactivity, structural stability and no fluidization problems. It is also an active catalyst for certain reactions, such as decomposition of hydrocarbon.

Nickel-based oxygen carriers also involve disadvantages. Besides health issues and the high price, nickel comes with thermodynamic limitations and never allows 100 % conversion of any hydrocarbon-based fuel to CO<sub>2</sub> and H<sub>2</sub>O. Nickel is also known to suffer from poisoning/deactivation if it gets in contact with sulphur species at sufficient concentrations. The process is reversible, but only if the oxygen carrier is treated in a high temperature, sulphur-free atmosphere [14–16].

### 2.6. Conducted Experiments

Chemical-looping combustion experiments were conducted at temperatures between 750 °C and 900 °C and fuel flows corresponding to 144–578 W<sub>th</sub>. The amount of steam added was constant for all fuel flows and 0.75 ml<sub>liq</sub>/min. The operating conditions for the different experiments are summarized in Table 1, C1–C3.

Chemical-looping reforming experiments were carried out with the same oxygen carrier, reactor and equipment as were used for the combustion experiments. The fuel flow was varied between 289 W<sub>th</sub> and 982 W<sub>th</sub> and the air flow was 5.0–8.0 L<sub>n</sub>/min. The flow rate of steam was controlled by a steam generator to which 0.40–0.75 ml<sub>liq</sub>/min water was added, which corresponds to 0.50–0.95 L<sub>n</sub>/min steam. Key variables for chemical-looping reforming experiments are listed in Table 1, R1–R10.

Chemical-looping experiments with N4MZ-1400 under fuel addition were run for about 54 h, out of which 34 h were under combustion conditions and 20 h under reforming conditions.

## 3. Data Evaluation

### 3.1. Chemical-Looping Combustion

With the current measurement system carbon compounds are measured thoroughly. Hydrogen is only measured in pure form or in the form of lower hydrocarbons, up to C<sub>3</sub>H<sub>8</sub>. Therefore, the evaluation of the combustion process will be based on the fate of carbon. The fractions of exiting carbon species are related to the flow of carbon into the fuel reactor. These are listed in Table 2 and the corresponding calculations are given in equations (8)–(12).

$$C_{AR} = \frac{\dot{n}_{CO_2,AR}}{\dot{n}_{C,fuel,in}} \quad (8)$$

$$C_{CO_2,FR} = \frac{\dot{n}_{CO_2,FR}}{\dot{n}_{C,fuel,in}} \quad (9)$$

$$C_{CO,FR} = \frac{\dot{n}_{CO,FR}}{\dot{n}_{C,fuel,in}} \quad (10)$$

$$C_{CH_4,FR} = \frac{\dot{n}_{CH_4,FR}}{\dot{n}_{C,fuel,in}} \quad (11)$$

$$C_{>CH_4,FR} = \frac{\sum_{m=1}^9 (m \cdot \dot{n}_{C_mH_n,FR}) - \dot{n}_{CH_4,FR}}{\dot{n}_{C,fuel,in}} \quad (12)$$

$\dot{n}_{C,fuel,in}$  is the total molar flow of carbon from kerosene into the reactor and  $\dot{n}_i$  is the molar flow of species  $i$  exiting the reactor. This way of evaluating the combustion process is possible by drawing a mass balance around the reactor system as a whole, i.e. air reactor and fuel reactor. A more compact way of evaluating the combustion process is by using the CO<sub>2</sub> yield, which is a single valued measure of how much carbon in the fuel reactor is fully oxidized to CO<sub>2</sub>. The CO<sub>2</sub> yield, expressed through  $\gamma_{CO_2}$ , neither takes gas leakage from fuel reactor to air reactor into account nor transport of solid carbon. Hence, the quantity in reaction (13) can only be called a yield if carbon loss to the air reactor is negligible or exclusively due to gas leakage. Furthermore, it is not differentiated by equation (13) how far the fuel is oxidized. The CO<sub>2</sub> yield is expressed as the molar flow of CO<sub>2</sub> that leaves the fuel reactor divided by the sum of all carbon that leaves the fuel reactor. This ratio can be rewritten with concentrations instead of molar flows, see equation (13).

$$\begin{aligned} \gamma_{CO_2} &= \frac{\dot{n}_{CO_2,FR}}{\dot{n}_{CO_2,FR} + \dot{n}_{CO,FR} + \sum_{m=1}^9 (m \cdot \dot{n}_{C_mH_n,FR})} \\ &= \frac{y_{CO_2,FR}}{y_{CO_2,FR} + y_{CO,FR} + \sum_{m=1}^9 (m \cdot y_{C_mH_n,FR})} \end{aligned} \quad (13)$$

### 3.2. Chemical-Looping Reforming

The performance of CLR experiments is expressed by a factor  $\psi$ , which describes the number of moles oxygen taken up by the product gas, compared to what would be needed for complete combustion.  $\psi$  can be calculated with expressions (14)–(17), from the oxygen-to-carbon molar ratio of fuel and products.  $(O/C)_{FR}$  refers to the actual gas from the fuel reactor,  $(O/C)_{fm}$  refers to the fuel mix, and  $(O/C)_{cc}$  refers to the gas composition that would have been obtained by complete combustion of the fuel. The number of moles H<sub>2</sub>O and C in the fuel mix, as well as the number of moles H<sub>2</sub>O and CO<sub>2</sub> produced during complete combustion, is given by the flows of steam and kerosene.

**Table 1:** Overview of CLC and CLR experiments with N4MZ-1400 oxygen carrier

Test number	Fuel flow FR (ml <sub>liq</sub> /min)	Steam flow FR (ml <sub>liq</sub> /min) (L <sub>n</sub> /min)		Air flow AR (L <sub>n</sub> /min)	T <sub>FR</sub> (°C)	(H/C) <sub>fm</sub> (-)	Corresponding power (W)	Operation time (min)
C1	0.25 – 1.00	0.75	0.93	8.0	900	7.7 – 3.3	144 – 578	635
C2	0.25 – 0.50	0.75	0.93	8.0	750	7.7 – 4.8	144 – 289	635
C3	0.50	0.75	0.93	8.0	800	4.8	289	450
R1	1.00	0.75	0.93	7.0	930	3.3	578	75
R2	1.15	0.40	0.50	5.0	950	2.5	665	95
R3	1.45	0.40	0.50	5.0	950	2.4	838	90
R4	1.70	0.40	0.50	5.0	950	2.3	982	35
R5	1.45	0.75	0.93	5.0	950	2.9	838	90
R6	1.70	0.75	0.93	5.0	950	2.7	982	90
R7	1.15	0.75	0.93	5.0	950	3.1	665	90
R8	0.50 – 1.70	0.75	0.93	6.0	950	4.8 – 2.7	289 – 982	300
R9	0.50 – 1.30	0.75	0.93	6.0	850	4.8 – 3.0	289 – 751	200
R10	1.40	0.75	0.93	5.0 – 8.0	930	2.9	809	120

**Table 2:** Carbon fate categories

C-Species	Symbol	Explanation
CO <sub>2</sub> in FR	C <sub>CO<sub>2</sub>,FR</sub>	Reaction product in case of complete oxidation
CO in FR	C <sub>CO,FR</sub>	Intermediate reaction product; hydrocarbons are fully reformed but only partially oxidized
CH <sub>4</sub> in FR	C <sub>CH<sub>4</sub>,FR</sub>	Intermediate reaction product; hydrocarbons are mostly reformed but not fully oxidized
>CH <sub>4</sub> in FR	C <sub>&gt;CH<sub>4</sub>,FR</sub>	Intermediate reaction product; hydrocarbons are not or partially reformed
CO <sub>2</sub> in AR	C <sub>AR</sub>	All carbon that gets into the air reactor is expected to be fully oxidized to CO <sub>2</sub> . Carbon can either get into the air reactor in the form of gas, by gas leakage from fuel reactor to air reactor, or as solid carbon from coke formation, which is transported into the air reactor by the global particle circulation. However, it is only possible to observe the sum of both effects.

$$\psi = \frac{(O/C)_{FR} - (O/C)_{fm}}{(O/C)_{cc} - (O/C)_{fm}} \quad (14)$$

$$(O/C)_{FR} = \frac{2 \cdot \dot{n}_{CO_2,FR} + \dot{n}_{H_2O,FR} + \dot{n}_{CO,FR}}{\dot{n}_{CO_2,FR} + \dot{n}_{CO,FR} + \sum_{m=1}^9 (m \cdot \dot{n}_{C_mH_n,FR})} \quad (15)$$

$$(O/C)_{fm} = \frac{\dot{n}_{H_2O,fm}}{\dot{n}_{C,fm}} \quad (16)$$

$$(O/C)_{cc} = \frac{\dot{n}_{H_2O,cc} + 2 \cdot \dot{n}_{CO_2,cc}}{\dot{n}_{CO_2,cc}} \quad (17)$$

A  $\psi$  of 1.0 means that sufficient oxygen has been added to the fuel mix via the oxygen carrier to oxidize it completely to CO<sub>2</sub> and H<sub>2</sub>O. For stoichiometric partial oxidation into CO and H<sub>2</sub>,  $\psi$  is 0.25 for methane and  $\approx 0.34$  for the kerosene used here.

In order for  $\psi$  to be useful for evaluating the results of a chemical-looping reforming experiment, there should be very high conversion of hydrocarbons and no or little formation of solid carbon, and the gas composition should be reasonably close to thermodynamic equilibrium. These criteria were fulfilled for the experiments conducted in this study. Under such circumstances, the H<sub>2</sub>O flow from the fuel reactor can be estimated by a species balance, see Rydén et al. [12] for a more detailed description of the used methodology.

The desired value of  $\psi$  for a chemical-looping reforming

process depends on factors such as reactor temperature, fuel, desired product composition and amounts of H<sub>2</sub>O or CO<sub>2</sub> added to the fuel reactor. For a chemical-looping reforming process with natural gas as fuel, a  $\psi$  in the order of 0.30–0.35 seems reasonable [17]. With kerosene, 0.40–0.45 would likely be more appropriate, else the overall process would not be self sustaining with heat.

### 3.3. Oxygen Carrier

One way to characterize an oxygen carrier is through the oxygen transfer capacity  $R_o$ , see equation (18), which depends on type and ratio of active and inert phase. It expresses the highest theoretical mass change between the state of complete oxidation,  $m_{OC,ox}$ , and full reduction,  $m_{OS,red}$ .

$$R_o = \frac{m_{OC,ox} - m_{OC,red}}{m_{OC,ox}} \quad (18)$$

The difference between the reduced form of N4MZ-1400 (Ni + MgO-ZrO<sub>2</sub>) and its most oxidized form (NiO + MgO-ZrO<sub>2</sub>) corresponds to an oxygen transfer capacity of 8.4 wt%. However, it is not always desirable to reach that value. The actual degree of reduction of the oxygen carrier can be described through the degree of oxidation  $X$ , see equation (19), and the degree of mass-based conversion  $\omega$ , see equation (20).

$$X = \frac{m_{OC} - m_{OC,red}}{m_{OC,ox} - m_{OC,red}} \quad (19)$$

$$\omega = \frac{m_{OC}}{m_{OC,ox}} = 1 + R_o \cdot (X - 1) \quad (20)$$

The degree of conversion of the solids cannot be determined explicitly during operation of the 300 W reactor, since removal of solids during operation is not possible. One way to obtain the actual reduction is to determine the amount of oxygen needed to oxidize the oxygen carrier when the fuel flow is shut off. This so called reoxidation is usually performed at the end of each experiment.

It is possible to calculate the oxygen carrier circulation  $\dot{m}_{OC}$ , see equation (21), as a function of  $\omega$ , the oxygen consumed in the air reactor  $\Delta\dot{m}_{O_2,AR}$  and the degree of mass-based conversion in the air reactor  $\omega_{AR}$ . Here,  $\omega$  is derived from reoxidation data, see equation (20), and the oxygen consumption in the air reactor  $\Delta\dot{m}_{O_2,AR}$  from continuous CLC operation. If it is assumed that the oxygen carrier is completely oxidized to NiO in the air reactor during CLC operation, then  $\omega_{AR}$  in equation (21) becomes 1. Hence, the oxygen carrier circulation can be estimated for the one air reactor air flow, which was used prior to the reoxidation.

$$\dot{m}_{OC} = \frac{\omega_{AR} \cdot \Delta\dot{m}_{O_2,AR}}{\Delta\omega} = \frac{\omega_{AR}^{AR} \cdot \Delta\dot{m}_{O_2,AR}}{\omega_{AR}^{AR} - \omega} \quad (21)$$

The attrition rate was calculated from a simple exponential decay equation, based on the experimental time with fuel addition, the amount of recovered fines and the total recovered bed mass. Particles are hereby assumed to decay evenly over the whole experiment time, which is a simplified assumption. Here, fines are defined as particles with a diameter less than 45  $\mu\text{m}$ .

## 4. Results and Discussion

### 4.1. Chemical-Looping Combustion Experiments

Figure 6 shows the measured dry-gas concentration during experiment C1 with 289  $W_{th}$  fuel equivalent, cf. Table 1. The concentration of hydrogen, H<sub>2</sub> (WGS), was calculated under the assumption that the equilibrium of the water-gas shift reaction is valid. This assumption was supported by gas chromatograph measurements, H<sub>2</sub> (GC).

Due to thermodynamic limitations, nickel-based oxygen carriers cannot fully convert H<sub>2</sub> and CO into H<sub>2</sub>O and CO<sub>2</sub>. The calculated equilibrium concentrations for CO and H<sub>2</sub>, CO (eq.) and H<sub>2</sub> (eq.), are displayed in Figure 6 and show the lower limit of both species. Both concentrations were calculated for a hydrogen-to-carbon ratio of 5.1, a temperature of 900 °C and corrected for the balance gases, nitrogen and argon. Argon was used for all experiments to fluidize the loop-seals, and the presence of nitrogen was a result of a minor leakage from air reactor to fuel reactor. The measured dry-gas concentration of nitrogen in the fuel reactor was about 2 % for most experiments. 4 %,

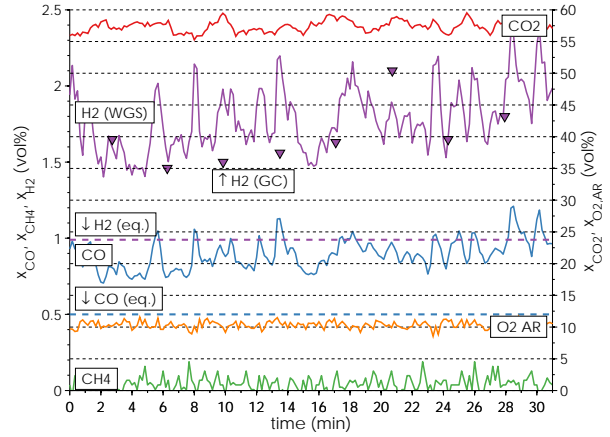


**Figure 6:** Dry-gas concentrations during chemical-looping combustion at  $T_{FR} = 900\text{ °C}$  with 289  $W_{th}$  (0.5  $\text{ml}_{liq}/\text{min}$ ) fuel and 0.75  $\text{ml}_{liq}/\text{min}$  H<sub>2</sub>O (H/C = 5.1). The balance is Ar, which was used to fluidize the loop-seals and about 4 % of N<sub>2</sub>, which leaked from AR to FR. The wet flue gas consisted of about 60 % H<sub>2</sub>O. The AR was fluidized with 8.0  $\text{L}_n/\text{min}$  air.

which was measured in this experiment, seems to be an exception and rather high. About half the oxygen that was provided by the air flow in the air reactor was transported into the fuel reactor with the oxygen carrier. For an industrial CLC unit, almost all the oxygen should be used so that only a few percent remain in the exhaust gases of the air reactor. The average CH<sub>4</sub> concentration was below 0.1 %. CO and H<sub>2</sub> differ only by 0.4 %-points and 0.8 %-points from the equilibrium values of 0.5 % and 1.0 %. Thus, the combustion was nearly complete.

Figure 7 shows the carbon conversion during the experiments; 7a and 7b show the effect of varied temperature, whereas 7c shows a varied fuel flow. Generally, the conversion was very good and nearly complete. The CO<sub>2</sub> yield was above 95 % at all times. The unconverted gases were mainly CO and H<sub>2</sub>, which is not shown here. No noteworthy concentrations of CH<sub>4</sub> or higher hydrocarbon were observed. The high but incomplete conversion of fuel was expected and can be ascribed to the thermodynamic limitations that apply to all nickel-based oxygen carriers. Thermodynamically, fuel conversion to CO<sub>2</sub> and H<sub>2</sub>O should decrease at higher temperature. The fact that the opposite is observed suggests that the oxidation of fuel is predominated by reaction kinetics, which generally improves at higher temperature, rather than thermodynamic equilibrium. When the fuel flow was varied at a constant air flow, the amount of oxygen available per unit of fuel changed. Higher oxygen-to-fuel ratios resulted in a higher conversion of fuel to CO<sub>2</sub> and H<sub>2</sub>O.

Between 4 % and 14 % of the ingoing carbon ended up in the air reactor. This observed carbon leak could be the result of both gas leakage and transport of solid carbon with the particle circulation. The latter is believed to be relevant, because nickel is known to favour coke formation at certain conditions. On the other hand, steam is known to suppress carbon formation. Furthermore, during earlier experiments with the here used reactor system, similar oxygen carrier particles and natural gas as fuel,

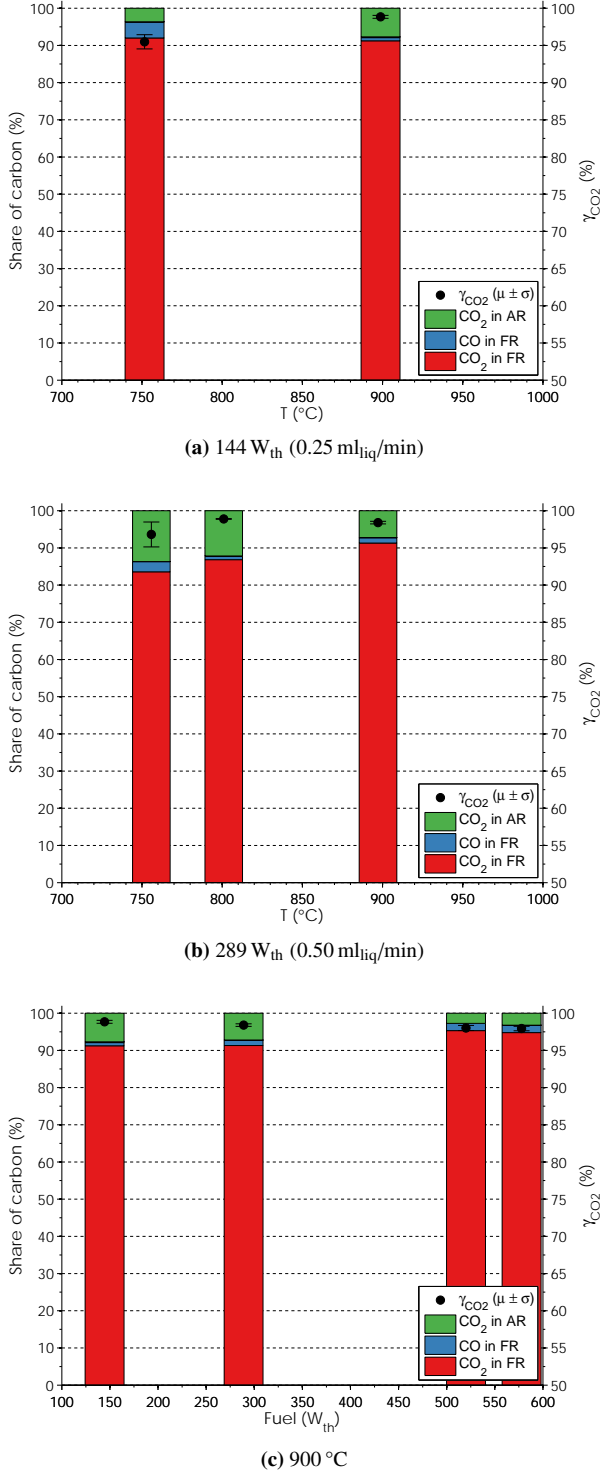


**Figure 7:** Carbon fate and CO<sub>2</sub> yield for CLC experiments with N4MZ-1400 for (a) 144 W<sub>th</sub> at different temperatures, (b) 289 W<sub>th</sub> at different temperatures and (c) at 900 °C with varied fuel flow

it was found that about 4–20% of the incoming fuel reactor flow leaked into the air reactor [12]. Hence, it is suspected that the CO<sub>2</sub> observed in the air reactor is mainly due to gas leakage. If that is the case then virtually all fuel carbon could be

captured as CO<sub>2</sub> in a properly sealed CLC system. It should be mentioned that no carbon leakage has been seen in larger units with gaseous fuel [18, 19]. This could be different with liquid fuels, but no safe conclusions can be drawn from the present experiments.

#### 4.2. Chemical-Looping Reforming Experiments

Syngas production was achieved by reducing the air-to-fuel ratio below the stoichiometric requirement for combustion. In this way, complete reoxidation of the oxygen carrier was prevented, and eventually there was too little oxygen available in the oxygen carrier to convert the fuel into CO<sub>2</sub> and H<sub>2</sub>O, see Figure 8 for an example.

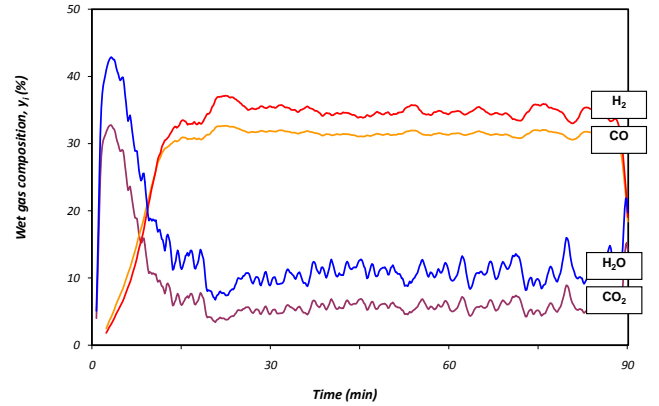


**Figure 8:** Wet-gas concentrations during chemical-looping reforming at  $T_{FR} = 950$  °C with 250 g N4MZ-1400 and an air factor of 0.40, fuel flow of 1.45 ml<sub>liq</sub>/min, steam flow of 0.40 ml<sub>liq</sub>/min and air flow of 5.0 L<sub>n</sub>/min. The concentration of CH<sub>4</sub> during the experiment was  $\approx 0.05$ %. The balance is Ar, which was used as fluidization gas in the particle seals.

In Figure 8, it can be seen that the kerosene initially was almost completely oxidized to CO<sub>2</sub> and H<sub>2</sub>O. This was possible since excess oxygen was stored in the fully oxidized oxygen carrier particles. However, since the oxygen added to the air reactor was insufficient to reoxidize the oxygen carrier, the overall degree of oxidation of the particles in the system slowly decreased, which resulted in a gradual shift of products towards CO and H<sub>2</sub>. In the example presented in Figure 8, steady state is achieved after about 15 min.

In Table 3,  $f_{CH_4}$  is the amount of CH<sub>4</sub> left in the synthesis gas compared to the amount carbon that was added to the reactor, expressed in %.  $\psi_{set}$  corresponds to the amount of air added to the air reactor compared to what is needed for complete combustion of the fuel.  $\psi_{real}$  is the corresponding number calculated from the composition of the fuel reactor gas according to equations (14)–(17). In Table 3, it can be seen that  $\psi_{real}$  typically differs somewhat from  $\psi_{set}$ . This is most apparent for experiment R1 for which  $\psi_{real}$  is much lower than  $\psi_{set}$ . The reason is that a comparably high air flow was used here and the outlet gas from the air reactor contained 7–8 vol% O<sub>2</sub>. This was the first reforming experiment conducted, so the process parameters had not yet been correctly established. For the following

**Table 3:** Results of chemical-looping reforming experiments with N4MZ-1400 oxygen carrier

Test number	$\psi_{\text{set}}$ (%)	$\psi_{\text{real}}$ (%)	$f_{\text{CH}_4}$ (%)
R1	91.7	54.7	0.01
R2	50.2	53.1	0.07
R3	39.8	40.4	0.05
R4	33.9	30.7	0.21
R5	39.8	43.1	0.02
R6	34.0	37.6	0.06
R7	50.2	54.6	0.01
R8	–	–	–
R9	–	–	–
R10	–	–	–

experiments, the air flow was reduced so that the  $\text{O}_2$  concentration from the air reactor became zero. For these instances,  $\psi_{\text{real}}$  typically was rather close to  $\psi_{\text{set}}$ . The minor deviations seen are likely due to uncertainties concerning the steam content in wet gas, which is estimated by thermodynamic equilibrium calculations rather than measured directly. The minor formation of solid char discussed below also has a small effect. The numbers in Table 3 are averages for each experimental period. Hence no numbers are shown for experiments R8 – R10, cf. Table 3, since varying operational parameters were used here.

In general, it can be said that the chemical-looping reforming experiments worked well. The reactor was operated at  $\psi_{\text{real}}$  between 0.30 and 0.55 and temperatures of 850 – 950 °C, which should be attractive conditions from an industrial point of view. The conversion of hydrocarbons into syngas was  $\approx 99.99\%$  for  $\psi = 0.50$  and  $\approx 99.90\%$  for  $\psi = 0.40$  at 950 °C. The selectivity towards  $\text{H}_2$  and  $\text{CO}$  was high, although the  $\text{H}_2$  concentration did not quite reach equilibrium for higher fuel flows. Small amounts of solid carbon accumulated in the reactor during operation, ranging from 0 – 1 % of the total amount of carbon added with the fuel during a time period of 70 – 300 min. Further, a  $\text{CO}_2$  concentration of roughly 0.5 vol% was measured after the air reactor. This corresponds to less than 2% of the carbon added to the fuel reactor and is believed to have been due to gas leakage. The one differing experiment was R4, for which the  $\text{CO}_2$  concentration after the air reactor was 1.5 vol%. This suggests larger gas leakage for this particular experiment, or more likely that the low air factor used in this experiment resulted in char formation in the fuel reactor. The char formed then followed the solids circulation to the air reactor in which it was combusted, resulting in slightly higher  $\text{CO}_2$  measured concentration. This is believed to have been reactor specific phenomena, see [13] for further discussion. There were no problems with defluidization, agglomeration, etc. despite the sometimes harsh experimental conditions.

### 4.3. Oxygen Carrier Analysis

The analysis of the used particles was done after 34 h of CLC and 20 h of CLR, concluding with combustion experiments.

The experiments with N4MZ-1400 showed no problems with fluidization. The only observed issue was the rather large accumulation of material in particle filters and water seal.

The amount of fines produced during the experiments seemed to be constant and was rather high. Due to nearly complete fuel conversion and fuel flows above the design values of the reactor system, see Table 1, the gas velocity in the fuel reactor was at times approaching the terminal velocity of the oxygen carrier particles. This caused not only fines to be carried out of the reactor, but also a minor amount of intact particles. Due to a high amount of fines, the material was difficult to sieve. Nickel dust stuck to sieve meshes and sieve walls and was, unlike the fresh material, no longer pourable. The average attrition rate was 0.4 %/h, which corresponds to an average lifetime of about 250 h.

Figure 9 shows the freeze-granulated nickel-based oxygen carrier N4MZ-1400 before and after the experiments with liquid fuel in the 300 W reactor. Figure 9a shows particles from the same batch as the ones used here but from a different size fraction. It can be seen that the fresh particles are mostly uniformly spherical, as is typical for freeze-granulated particles, but there are also a few particles with smaller particles attached to them, or so called satellites. The smaller size fraction, which was used for the experiments in the 300 W reactor, is assumed to be more regular shaped, i.e. without such satellites. The used particles, which can be seen in Figure 9b, are still quite spherical, but it can clearly be seen that many particles are broken. No differences in surface structure were observed.

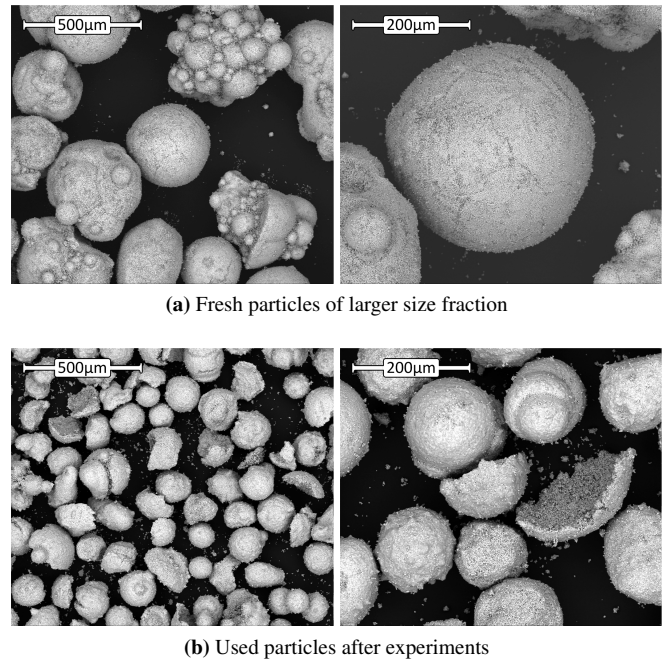
**Figure 9:** SEM images of nickel based oxygen carrier N4MZ-1400 (a) before and (b) after CLC and CLR experiments with liquid fuel

Table 4 shows the results of X-ray powder diffractometry (XRD) and BET surface area measurements of fresh and used N4MZ-1400 particles. The lower detection limit of XRD lies

at about 4 mol%. Here, an exact quantification was not possible. The indicated phases in Table 4 are listed after occurrence: more frequent phases are listed first.

**Table 4:** XRD and BET surface measurement of N4MZ-1400 particles after CLC experiments

Particles	Indicated phases by XRD	BET surface area (m <sup>2</sup> /g)
Fresh (> 212 μm)	ZrO <sub>2</sub> ( <i>m</i> ), NiO	0.6
Used (90–250 μm)	ZrO <sub>2</sub> ( <i>m</i> ), NiO, Ni	1.1
Used (< 45 μm)	ZrO <sub>2</sub> ( <i>m</i> ), NiO, Ni	–

(*m*) monoclinic crystal structure

A couple of things should be pointed out with respect to the identified phases. N4MZ-1400 is a synthesized oxygen carrier, which is designed so that the active phase, NiO, is mixed with an inert phase, ZrO<sub>2</sub>, in order to increase particle stability and thus lifetime. ZrO<sub>2</sub> has a high thermal resistance and mechanical strength. With an increasing temperature ZrO<sub>2</sub> undergoes phase changes. Below 1170 °C it has a monoclinic crystal structure, between 1170 °C and 2367 °C a tetragonal one and between 2367 °C and melting temperature 2690 °C it becomes cubic [20]. Each crystal structure has a different density, which increases in the order monoclinic → tetragonal → cubic. A phase transformation is thus accompanied by an abrupt volume change, which is likely to cause cracks in the particle structure. Although the phase-transformation temperatures lie well beyond temperatures where CLC and CLR experiments are conducted, the initial calcination can well happen in this temperature range. This means that such particles could a priori have a weakened structure. In order to avoid a phase transformation at high temperatures, ZrO<sub>2</sub> can be stabilized by mixing it with certain metal oxides whose ions diffuse at very high temperatures, about 1700 °C, into the crystal structure of ZrO<sub>2</sub>. Such so called stabilized ZrO<sub>2</sub> has a cubic structure at room temperature and does not undergo structural changes upon heating until the melting point is reached. In order to avoid cracking of particles due to initial heat treatment, it is important that ZrO<sub>2</sub> is stabilized both, homogeneously and completely. Such a structure is called fully stabilized ZrO<sub>2</sub> in contrast to partially stabilized ZrO<sub>2</sub>. In order to fully stabilize ZrO<sub>2</sub> with MgO, about 15 mol–30 mol% MgO have to be mixed with ZrO<sub>2</sub> at high temperatures [21].

N4MZ-1400 was supposed to consist of partially or fully stabilized ZrO<sub>2</sub>, which was necessary due to its high calcination temperature. The fact that neither cubic ZrO<sub>2</sub> nor MgO were found indicates that the ZrO<sub>2</sub> was not fully stabilized as intended. This might be the cause for the unexpectedly high attrition rate of N4MZ-1400.

The presence of minor amounts of metallic nickel in the used particle samples indicates that the active nickel phase could not be fully oxidized. Hence, the oxygen transfer capacity is reduced. On the other hand, metallic nickel is known to catalyze certain reactions in the fuel reactor, such as hydrocarbon decomposition. However, after an initial phase with fresh particles, where the fuel conversion clearly improved with time and

which took about 1 h, neither degradation nor improvement in fuel conversion were noted.

The measured BET surface area of the used particles is almost twice as high as that of fresh particles, see Table 4. However, since both values are quite low, this increase in surface area could be partly explained by the difference in particle size between fresh and used particles.

Besides the obvious carbon transport to the air reactor, see Figure 7, there seems to be no further noteworthy carbon deposition in the fuel reactor during fuel addition. After the experiments the circulation was stopped so that the reduced particles stayed in the fuel reactor. When thereupon the particles were reoxidized by air, some CO<sub>2</sub> was detected. The carbon in the CO<sub>2</sub> corresponded to less than 0.1 % of the total amount of carbon added earlier through the fuel. At least part of that carbon was on the particles and would have been transported into the air reactor, meaning that the actual amount of carbon that was deposited in the fuel reactor was even smaller.

The global particle circulation could be estimated for the combustion experiments C1–C3. The measured  $\Delta\omega$  for an air flow of 8.0 L<sub>n</sub>/min was 3–6 %, which corresponds to  $\Delta X$  of 29–64 %. The resultant particle circulation is 0.3–0.7 g/s or, when divided by the cross-sectional area of the fuel reactor, 5–11 kg/s m<sup>2</sup>.

## 5. Conclusions

This paper provides a proof of concept of CLC and CLR with a liquid fuel in a directly fired unit with continuous circulation. The nickel-based oxygen carrier that was used turned out to have very good fuel conversion properties, but a noteworthy fraction of the particles broke down to a size below 45 μm. This integrity issue is believed to be caused by the fact that the magnesium-stabilized zirconium dioxide, which was used as stabilizing agent, was in fact not fully stabilized. Hence, the particles would have been partially fractured during the initial calcination.

The fuel conversion to H<sub>2</sub>O and CO<sub>2</sub> during chemical-looping combustion was high but incomplete. The CO<sub>2</sub> yield was as high as 99 % and never below 95 %. The amount of H<sub>2</sub> and CO left in the fuel reactor gases came very close to the calculated equilibrium concentrations. The amount of CH<sub>4</sub> left in the fuel reactor gases did not exceed 0.2 % in dry-gases. No other hydrocarbons were detected. One issue that occurred was carbon transport to the air reactor. As much as 14 % of the fuel carbon leaked into the air reactor and was thus lost to the carbon sequestration. However, the carbon leakage is at least partly ascribed to the reactor specific gas leakage from fuel reactor to air reactor.

During the chemical-looping reforming experiments nearly all hydrocarbon could be reformed into a synthesis gas, which consisted mainly of CO and H<sub>2</sub>. In the best case, only 0.01 % of the fuel carbon remained as hydrocarbon.

Generally, chemical-looping combustion and chemical-looping reforming experiments went very well and showed a performance, similar to gaseous fuels.

## Nomenclature

### Latin symbols

$f_{\text{CH}_4}$	[-]	CH <sub>4</sub> fraction in synthesis gas compared to added carbon
$m$	[kg]	mass
$\dot{m}_{\text{OC}}$	[kg/s]	oxygen carrier circulation
$\dot{n}$	[mol/s]	molar flow
$x$	[vol%]	dry-gas concentration
$y$	[vol%]	wet-gas concentration
$C$	[-]	carbon fraction
H/C	[-]	hydrogen-to-carbon ratio
$R_o$	[wt%]	oxygen transfer capacity
$S_{\text{BET}}$	[m <sup>2</sup> /g]	BET surface area
$T$	[°C] or [K]	temperature
$T_{\text{boil}}$	[°C] or [K]	boiling temperature
$X$	[%]	degree of oxidation

### Greek symbols

$\gamma_{\text{CO}_2}$	[%]	CO <sub>2</sub> gas yield
$\mu$	varies	mean value
$\rho_{\text{bulk}}$	[g/cm <sup>3</sup> ]	bulk density
$\sigma$	varies	standard deviation
$\psi$	[-]	degree of oxidation of fuel
$\omega$	[%]	degree of mass-based conversion

### Indices

( ) <sub>cc</sub>	complete combustion
( ) <sub>fm</sub>	fuel mix
( ) <sub>in</sub>	at the reactor inlet
( ) <sub>ox</sub>	most oxidized state
( ) <sub>red</sub>	most reduced state
( ) <sub>AR</sub>	air reactor
( ) <sub>FR</sub>	fuel reactor
( ) <sub>OC</sub>	oxygen carrier

### Acronyms

AR	air reactor
CLC	chemical-looping combustion
CLR	chemical-looping reforming
FR	fuel reactor
GC	gas chromatograph
N4MZ-1400	40 wt% NiO on 60 wt% MgO-ZrO <sub>2</sub> calcined at 1400 °C
OC	oxygen carrier
SEM	scanning electron microscopy
XRD	X-ray powder diffractometry

## Acknowledgements

The study is carried out under the project ‘‘Chemical-looping with liquid hydrocarbon fuels’’ financed by Saudi Aramco. The authors would also like to thank Harald Jeppsson from Preem AB for providing the kerosene. A special thanks to Sven-Ingvar Andersson for conduction fuel analysis and helping with his expertise.

## References

- [1] M. M. Hossain, H. I. de Lasa, Chemical-looping combustion (CLC) for inherent CO<sub>2</sub> separations—a review, *Chemical Engineering Science* 63 (18) (2008) 4433–4451.
- [2] H. Fang, L. Haibin, Z. Zengli, Advancements in Development of Chemical-Looping Combustion: A Review, *International Journal of Chemical Engineering* 2009 (2009) 16.
- [3] A. Lyngfelt, Oxygen carriers for chemical-looping combustion – 4000 h of operational experience, *Oil & Gas Science and Technology* 66 (2) (2011) 161–172.
- [4] P. Pimenidou, G. Rickett, V. Dupont, M. Twigg, Chemical looping reforming of waste cooking oil in packed bed reactor, *Bioresource Technology* 101 (16) (2010) 6389–6397.
- [5] P. Pimenidou, G. Rickett, V. Dupont, M. Twigg, High purity H<sub>2</sub> by sorption-enhanced chemical looping reforming of waste cooking oil in a packed bed reactor, *Bioresource Technology* 101 (23) (2010) 9279–9286.
- [6] Y. Cao, B. Lia, H.-Y. Zhao, C.-W. Lin, S. P. Sit, W.-P. Pan, Investigation of Asphalt (Bitumen)-fuelled Chemical Looping Combustion using Durable Copper-based Oxygen Carrier, *Energy Procedia* 4 (2011) 457–464, greenhouse Gas Control Technologies 10.
- [7] A. Forret, A. Hoteit, T. Gauthier, Chemical Looping Combustion Process applied to liquid fuels, in: *British – French Flame Days*, Lille, France, 37–37, 2009.
- [8] A. Hoteit, A. Forret, W. Pelletant, J. Roesler, T. Gauthier, Chemical Looping Combustion with Different Types of Liquid Fuels, *Oil & Gas Science and Technology – Reb IFP Energies nouvelles* 66 (2) (2011) 193–199.
- [9] T. Mendiara, J. M. Johansen, R. Utrilla, P. Geraldo, A. D. Jensen, P. Glarborg, Evaluation of different oxygen carriers for biomass tar reforming (I): Carbon deposition in experiments with toluene, *Fuel* 90 (3) (2011) 1049–1060.
- [10] A. Lyngfelt, B. Leckner, T. Mattisson, A fluidized-bed combustion process with inherent CO<sub>2</sub> separation; application of chemical-looping combustion, *Chemical Engineering Science* 56 (2001) 3101–3113.
- [11] M. Rydén, A. Lyngfelt, T. Mattisson, Synthesis gas generation by chemical-looping reforming in a continuously operating laboratory reactor, *Fuel* 85 (12-13) (2006) 1631–1641.
- [12] M. Rydén, A. Lyngfelt, T. Mattisson, Chemical-looping combustion and chemical-looping reforming in a circulating fluidized-bed reactor using Ni-based oxygen carriers, *Energy & Fuels* 22 (2008) 2585–2597.
- [13] M. Rydén, M. Johansson, A. Lyngfelt, T. Mattisson, NiO supported on Mg-ZrO<sub>2</sub> as oxygen carrier for chemical-looping combustion and chemical-looping reforming, *Energy and Environmental Science* 2 (9) (2009) 970–981.
- [14] T. Mattisson, M. Johansson, A. Lyngfelt, The use of NiO as an oxygen carrier in chemical-looping combustion, *Fuel* 85 (5-6) (2006) 736–747.
- [15] F. García Labiano, L. F. de Diego, P. Gayán, J. Adánez, A. Abad, C. Dueso, Effect of Fuel Gas Composition in Chemical-Looping Combustion with Ni-Based Oxygen Carriers. 1. Fate of Sulfur, *Industrial & Engineering Chemistry Research* 48 (5) (2009) 2499–2508.
- [16] L. Shen, Z. Gao, J. Wu, J. Xiao, Sulfur behavior in chemical looping combustion with NiO/Al<sub>2</sub>O<sub>3</sub> oxygen carrier, *Combustion and Flame* 157 (5) (2010) 853–863.
- [17] M. Rydén, A. Lyngfelt, Hydrogen and power production with integrated carbon dioxide capture by chemical-looping reforming, in: E. Rubin, D. Keith, C. Gilboy, M. Wilson, T. Morris, J. Gale, K. Thambimuthu (Eds.), *Greenhouse Gas Control Technologies* 7, Elsevier Science Ltd, Oxford, 125–134, 2005.
- [18] C. Linderholm, A. Abad, T. Mattisson, A. Lyngfelt, 160 h of chemical-looping combustion in a 10kW reactor system with a NiO-based oxygen carrier, *International Journal of Greenhouse Gas Control* 2 (4) (2008) 520–530.
- [19] C. Linderholm, T. Mattisson, A. Lyngfelt, Long-term integrity testing of spray-dried particles in a 10-kW chemical-looping combustor using natural gas as fuel, *Fuel* 88 (11) (2009) 2083–2096.
- [20] D. Marshall, R. Hannink, Ceramics: Transformation Toughening, in: K. H. J. Buschow, R. W. Cahn, M. C. Flemings, B. I. (print), E. J. Kramer, S. Mahajan, P. V. (updates) (Eds.), *Encyclopedia of Materials: Science and Technology*, Elsevier, Oxford, 1113–1116, 2001.
- [21] T. Etsell, S. Flengas, Electrical Properties of Solid Oxide Electrolytes, *Chemical Reviews* 70 (3) (1970) 339–376.